Neutron Diffraction Studies on the Hydrogen-Bonded Structure in Concentrated Aqueous Hydrochloric Acid Solutions

Yasuo Kameda,* Takeshi Usuki, and Osamu Uemura

Department of Material and Biological Chemistry, Faculty of Science, Yamagata University, Kojirakawa-machi 1-4-12, Yamagata 990-8560

(Received December 5, 1997)

The neutron diffraction measurement with the H/D isotopic substitution technique has been carried out on the aqueous 21 mol% hydrochloric acid solutions, in order to investigate the short-range structure in the concentrated aqueous acid solution, in comparison with the structural information available on liquid pure water. Observed partial structure factors: $a_{HH}(Q)$, $a_{XH}(Q)$, and $a_{XX}(Q)$ (X: O, Cl), determined by the least-squares fitting analysis, have exhibited that the nearest-neighbor intermolecular hydrogen-bond distances, r(H···H) and r(O···H), between oxonium ion and water molecule in the 21 mol% hydrochloric acid solution were 2.02±0.05 and 1.69±0.02 Å, respectively; such values are much smaller than those in liquid pure water. Consequently, a strong intermolecular hydrogen bond between oxonium ion and its nearest-neighbor water molecules is concluded to be present in the concentrated aqueous hydrochloric acid solution.

The elucidation of the solvation structure around H_3O^+ in the aqueous solution is indispensable for understanding the mechanism of the proton transfer reaction, which plays an important role in various chemical and biological processes.[1] Previous X-ray diffraction studies for concentrated aqueous hydrochloric acid solutions have indicated that the hydrogen-bond distance between H_3O^+ and its nearest-neighbor H_2O molecules is quite short (2.56 Å,[2] 2.5—2.6 Å,[3] 2.44 Å[4]) compared with that reported for pure liquid water (2.85 Å[5—14]). Triolo and Narten have analyzed in detail the hydration structure of H_3O^+ combining X-ray and neutron diffraction data; they postulated that H_3O^+ has the tetrahedral hydration structure, in which one of neighboring H_2O molecules points its O atom toward the O atom of the central H_3O^+.[5] However, this structural model seems to be unlikely from the point of view of the electrostatistics. Theoretical studies by molecular orbital (MO)[15—20] and molecular dynamics (MD)[21—23] simulations have recently focused upon the proton transfer reaction in the aqueous acidic solution. For example, the ab initio MO calculation for protonated water clusters, $H_3O^+(H_2O)_n$, by Komatsuzaki and Ohmine, has pointed out that the proton transfer reaction goes on in spite of barriers with a small potential energy of only a few kcal/mol or less.[20] The ab initio MD study by Lobaugh and Voth[22] has suggested that the shorter O···O distance in the aqueous acid solution observed by X-ray diffraction studies is attributed to that within protonated water dimer, $H_5O_2^+$. The idea that $H_5O_2^+$ is a dominant species in concentrated aqueous acidic solution, has recently been suggested by Agmon, who gave a reasonable interpretation of the results observed by previous diffraction and spectroscopic studies.[24,25] On the other hand, Laasonen and Klein have proposed that hydrogen-bonded species such as Cl–H···Cl^- are formed in the concentrated aqueous hydrochloric acid solution with $HCl/H_2O = 1/3.6$.[23] Consequently, further structural information of the partial structure function experimentally obtained is necessary for elucidating the solvation structure of H_3O^+ in the concentrated aqueous acidic solution.

The neutron diffraction experiment with the H/D isotopic substitution technique is one of the most desirable methods to solve the problem. In the present paper, we describe results of the neutron diffraction measurement for three aqueous 21 mol% hydrochloric acid solutions with different H/D isotopic compositions. We discuss the intermolecular hydrogen-bonded structure in the highly concentrated aqueous solution through the comparison of partial structure functions for the solutions and for liquid pure water.

Experimental and Data Analysis

Materials. Weighed amounts of concentrated DCl–D_2O (99.5% D, Aldrich Chemical Inc., Co.) and HCl–H_2O (Nacalai tesque, Guaranteed grade) solutions were mixed to prepare three aqueous 21 mol% *HCl solutions with different H/D isotopic compositions, (99.5% D, 35.9% D, and 67.7% D, respectively). The concentration of each sample was checked by the standard acid-base titration. Liquid pure water samples with different H/D ratios were also prepared by mixing weighed amounts of D_2O (99.9% D, Aldrich Chemical Inc., Co.) and distilled H_2O. These samples were sealed into a cylindrical quartz cell (11.4 mm in inner diameter and 1.2 mm in thickness). Sample parameters are listed in Table 1. The coherent scattering length, scattering and absorption cross sections for nuclei, O and Cl, were derived from the corresponding values tabulated by Sears.[26] The scattering cross sections for H and D nuclei calculated from observed total cross sections for liquid H_2O and D_2O,[27,28] were applied to the absorption correction for diffraction intensities. The sample with the isotopic composition of the "null mixture", in which the mean scattering length of H is zero, was prepared with the purpose of depressing enhanced uncertainties due to extremely large incoherent scattering of H in the data

Table 1. Isotopic Compositions, Mean Scattering Lengths, b_H, for Hydrogen Atom, Total Cross-Sections, and the Number Density Scaled in the Stoichiometric Unit $(^*HCl)_x(H_2O)_{1-x}$, σ_t, and ρ_0, Respectively, for Sample Solutions Used in This Study

Samples	H/%	D/%	$b_H/10^{-12}$ cm[a]	σ_t/barns[b]	ρ/Å^{-3}
$(DCl)_{0.21}(D_2O)_{0.79}$	0.5	99.5	0.662	21.45	
$(^0HCl)_{0.21}(^0H_2O)_{0.79}$[c]	64.1	35.9	0	55.26	0.0323
$(^{0\text{-}2}HCl)_{0.21}(^{0\text{-}2}H_2O)_{0.79}$	32.3	67.7	0.331	38.35	
D_2O	0.1	99.9	0.666	12.45	
^0H_2O	64.1	35.9	0	50.47	0.0333
$^{0\text{-}2}H_2O$	32.1	67.9	0.333	31.46	

a) Taken from Ref. 26. b) Calculated using total cross sections of D_2O and H_2O[27,28] for the incident neutron wavelength of 0.999 Å. c) The superscript 0 denotes the isotopic mixture with $b_H = 0$.

correction procedure.

Neutron Diffraction Measurements. The neutron diffraction measurement was carried out at 25 °C using the ISSP diffractometer (PANSI) at the JRR-2 reactor operated at 10 MW in The Japan Atomic Energy Research Institute, Tokai, Japan. The incident neutron wavelength, $\lambda = 0.999 \pm 0.006$ Å, was determined by Bragg reflections from the KCl powder. Collimations used were 40′—40′ in going from the reactor to the detector. The aperture of the collimated beam was 20 mm in width and 40 mm in height. Scattered neutrons from the sample were collected in the BF_3 proportional counter over the angular range of $3 \leq 2\theta \leq 102°$, corresponding to the scattering vector magnitude range of $0.33 \leq Q \leq 9.78$ Å^{-1} ($Q = 4\pi \sin\theta/\lambda$). The step interval was chosen to be $\Delta(2\theta) = 0.5°$ in the range of $3 \leq 2\theta \leq 40°$ and $\Delta(2\theta) = 1.0°$ in the range of $41 \leq 2\theta \leq 102°$, respectively. The preset time was 240—360 s. Scattering intensities from the vanadium rod (10 mm in diameter), empty cell and background, were measured in advance.

Data Analysis. The measured scattering intensities were corrected for the background scattering and absorptions of both the sample and cell.[29] The count rate of the sample observed was converted to the absolute scale by the use of scattering intensities from the vanadium rod.

Although several theoretical approaches have been proposed in the literature,[30—36] no generalized procedure seems to be established for the multiple and inelasticity scattering correction in the aqueous solutions involving $^*H_2O$ and $^*H_3O^+$, such as the present sample. Previous Monte-Carlo calculations have indicated that observed scattering intensities in the liquid formic acid containing a considerable amount of H depend markedly on Q, reflecting the strong Q-dependence of the multiple scattering term.[31] The present samples exhibit also strong Q-dependent scattering intensities owing to the inelasticity effect of H, that is to say, they decrease with increasing 2θ. Then, since it is difficult to evaluate the multiple scattering contribution for the present sample adequately by a simple isotropic approximation of Blech and Averbach,[30] we employ in the present study the empirical method of the polynomial expansion which has been frequently applied to the data correction for samples containing complexed molecules, such as liquid methanol,[37,38] ethanol,[39] and D-glycerol.[40] More recently, Bellicent-Funel et al. have indicated that the polynomial expansion method supplies reliable inelasticity corrections for liquid D_2O and D_2O/H_2O mixtures.[41]

Observed total scattering intensities, $(d\sigma/d\Omega)^{obs}$, involving coherent, incoherent and multiple scattering contributions can be approximated by the following equation:

$$(d\sigma/d\Omega)^{obs} = \alpha[(d\sigma/d\Omega)_{int}^{intra} + (d\sigma/d\Omega)_{int}^{inter} + (d\sigma/d\Omega)^{self}], \quad (1)$$

where α is the normalization factor, in which the uncertainty in the absorption correction is included. $(d\sigma/d\Omega)_{int}^{intra}$ and $(d\sigma/d\Omega)_{int}^{inter}$ stand for intra- and intermolecular interference terms relating to the liquid structure. $(d\sigma/d\Omega)_{int}^{intra}$ is represented by two contributions from $^*H_2O$ molecule and $^*H_3O^+$, i.e.,

$$(d\sigma/d\Omega)_{int}^{intra} = (1-2x)(d\sigma/d\Omega)_{int}^{intra}(\text{for } ^*H_2O) + x(d\sigma/d\Omega)_{int}^{intra}(\text{for } ^*H_3O^+), \quad (2)$$

where

$$(d\sigma/d\Omega)_{int}^{intra}(\text{for } ^*H_2O) = 4b_O b_H \exp(-l_{OH}^2 Q^2/2)\sin(Qr_{OH})/(Qr_{OH}) + 2b_H^2 \exp(-l_{HH}^2 Q^2/2)\sin(Qr_{HH})/(Qr_{HH}), \quad (3)$$

and

$$(d\sigma/d\Omega)_{int}^{intra}(\text{for } ^*H_3O^+) = 6b_O b_H \exp(-l'^2_{OH} Q^2/2)\sin(Qr'_{OH})/(Qr'_{OH}) + 6b_H^2 \exp(-l'^2_{HH} Q^2/2)\sin(Qr'_{HH})/(Qr'_{HH}). \quad (4)$$

The self term in Eq. 1 can be expanded in the following manner as a polynomial function of Q:

$$(d\sigma/d\Omega)^{self} = (d\sigma/d\Omega)^{coh} + (d\sigma/d\Omega)^{inc} + (d\sigma/d\Omega)^{multi} = A + BQ^2 + CQ^4 + DQ^6 + EQ^8. \quad (5)$$

$(d\sigma/d\Omega)_{int}^{inter}$ decays much faster against Q than $(d\sigma/d\Omega)_{int}^{intra}$ because the former is composed by atomic pair correlations with larger internuclear distances and root mean square amplitudes. Then, the total $(d\sigma/d\Omega)^{obs}$ in the higher-Q region can be approximated as the sum of intramolecular and self scattering terms. Coefficients (A—E) in Eq. 5 are determined by the least-squares fitting procedure under the condition of minimizing the value of U defined below:

$$U = \int_{Q_{min}}^{Q_{max}} [(d\sigma/d\Omega)^{obs} - \alpha\{(d\sigma/d\Omega)_{int}^{intra} + (d\sigma/d\Omega)^{self}\}]^2 dQ. \quad (6)$$

Since the range of the observed scattering data is limited to $Q < 9.7$ Å^{-1} in the present study, the value of the upper limit of the integral, Q_{max}, is fixed at 9.7 Å^{-1}. The lower limit, Q_{min}, is chosen to be 3.0 Å^{-1} in the present analysis, considering the following criteria in determining a reliable $(d\sigma/d\Omega)_{int}^{inter}$ term.

1) Amplitude of the intermolecular term, $(d\sigma/d\Omega)_{int}^{inter}$, should be small in the Q-region above Q_{min}.

2) The low-Q limit of deduced $(d\sigma/d\Omega)_{int}^{inter}$ approaches to the theoretical value, $(\rho\chi_T k_B T - 1)\sum b_i^2 - (d\sigma/d\Omega)_{int}^{intra}$ (Q=0), where

χ_T and k_B denote the isothermal compressibility and the Boltzmann constant, respectively.

3) The value of the intermolecular distribution function, calculated by the Fourier transform of the $(d\sigma/d\Omega)_{int}^{inter}$ in the low-r region between r=0 and 1.5 Å, is minimized.

In the fitting procedure using the SALS program,[42] intramolecular parameters for H_2O molecule and H_3O^+ were fixed as follows : r_{OH}= 0.983 Å, l_{OH}=0.067 Å, r_{HH}=1.55 Å, l_{HH}=0.12 Å, r'_{OH}=1.04 Å, l'_{OH}=0.07 Å, r'_{HH}=1.63 Å and l'_{HH}=0.12 Å, respectively. These values have been referred from our previous neutron diffraction study.[43]

$(d\sigma/d\Omega)_{int}^{inter}$ is rewritten as the following equation:

$$(d\sigma/d\Omega)_{int}^{inter} = (d\sigma/d\Omega)^{obs}/\alpha - (d\sigma/d\Omega)_{int}^{intra} - (d\sigma/d\Omega)^{self}. \quad (7)$$

H–H, X–H, and X–X (X: O, Cl) partial structure factors, $a_{HH}(Q)$, $a_{XH}(Q)$, and $a_{XX}(Q)$, are respectively deduced from the combination of observed $(d\sigma/d\Omega)_{int}^{inter}$ terms, for three sample solutions : namely, $(DCl)_x(D_2O)_{1-x}$, $(^0HCl)_x(^0H_2O)_{1-x}$, and $(^{0\text{-}2}HCl)_x(^{0\text{-}2}H_2O)_{1-x}$. The superscript '0' denotes the null mixture for H atom. In the third solution, the isotopic composition of H atom has been chosen to be the average value of the first and second solutions, i.e., $b_{^{0\text{-}2}H}=(b_D+b_{^0H})/2$.

The intermolecular interference term, scaled by a stoichiometric unit, $(H_aCl)_x(H_{w2}O)_{1-x}$, can be written as the weighted sum of ten partial structure factors:

$$\begin{aligned}(d\sigma/d\Omega)_{int}^{inter} = {} & x^2 b_{Ha}^2[a_{HaHa}(Q)-1] + x^2 b_{Cl}^2[a_{ClCl}(Q)-1] \\ & +2x^2 b_{Ha}b_{Cl}[a_{ClHa}(Q)-1] \\ & +4x(1-x)b_{Ha}b_{Hw}[a_{HaHw}(Q)-1] \\ & +2x(1-x)b_{Ha}b_O[a_{OHa}(Q)-1] \\ & +4x(1-x)b_{Ha}b_{Cl}[a_{ClHa}(Q)-1] \\ & +2x(1-x)b_O b_{Cl}[a_{OCl}(Q)-1] \\ & +4(1-x)^2 b_{Hw}^2[a_{HwHw}(Q)-1] \\ & +4(1-x)^2 b_O b_{Hw}[a_{OHw}(Q)-1] \\ & +(1-x)^2 b_O^2[a_{OO}(Q)-1], \end{aligned} \quad (8)$$

where H_a and H_w denote the acidic and the water hydrogen, respectively. Since hydrogen atom is exchangeable between the oxonium ion and water molecule in the present solutions, the values of coherent scattering lengths in Eq. 8, b_{Ha} and b_{Hw}, should be identical. The hydrogen-hydrogen partial structure factor is obtained by the combination of observed $(d\sigma/d\Omega)_{int}^{inter}$ terms for three sample solutions which are identical in all details except for the H/D ratio:

$$\begin{aligned} & (d\sigma/d\Omega)_{int}^{inter}(\text{for D}) + (d\sigma/d\Omega)_{int}^{inter}(\text{for } ^0H) - 2(d\sigma/d\Omega)_{int}^{inter}(\text{for } ^{0-2}H) \\ & = x^2 b_D^2/2[a_{HaHa}(Q)-1] + 4x(1-x)b_D^2/2[a_{HaHw}(Q)-1] \\ & \quad +4(1-x)^2 b_D^2/2[a_{HwHw}(Q)-1] \\ & = (2-x)^2 b_D^2/2[a_{HH}(Q)-1], \end{aligned} \quad (9)$$

where

$$\begin{aligned} a_{HH}(Q)-1 = {} & x^2/(2-x)^2[a_{HaHa}(Q)-1] \\ & +4x(1-x)/(2-x)^2[a_{HaHw}(Q)-1] \\ & +4(1-x)^2/(2-x)^2[a_{HwHw}(Q)-1]. \end{aligned} \quad (10)$$

The observed $a_{HH}(Q)$ can be regarded as a weighed average of a_{HaHa}, a_{HaHw}, and a_{HwHw} terms. Similarly, the weighted sum of hydrogen–oxygen and hydrogen–chlorine partial structure factors can be deduced by combining the three observed intermolecular interference terms as follows:

$$\begin{aligned} & 4(d\sigma/d\Omega)_{int}^{inter}(\text{for } ^{0-2}H) - (d\sigma/d\Omega)_{int}^{inter}(\text{for D}) - 3(d\sigma/d\Omega)_{int}^{inter}(\text{for } ^0H) \\ & = 2x^2 b_D b_{Cl}[a_{ClHa}(Q)-1] + 4x(1-x)b_D b_{Cl}[a_{ClHw}(Q)-1] \\ & \quad +2x(1-x)b_D b_O[a_{OHa}(Q)-1] + 4(1-x)^2 b_D b_O[a_{OHw}(Q)-1] \\ & = 2(2-x)(1-x)b_O b_D[a_{OH}(Q)-1] + 2x(2-x)b_{Cl}b_D[a_{ClH}(Q)-1] \\ & = 2(2-x)\{(1-x)b_O + xb_{Cl}\}[a_{XH}(Q)-1], \end{aligned} \quad (11)$$

where

$$\begin{aligned} a_{ClH}(Q)-1 = {} & x/(2-x)[a_{ClHa}(Q)-1] \\ & +2(1-x)/(2-x)[a_{ClHw}(Q)-1], \end{aligned} \quad (12)$$

$$\begin{aligned} a_{OH}(Q)-1 = {} & x/(2-x)[a_{OHa}(Q)-1] \\ & +2(1-x)/(2-x)[a_{OHw}(Q)-1], \end{aligned} \quad (13)$$

and

$$\begin{aligned} a_{XH}(Q)-1 = {} & xb_{Cl}/\{(1-x)b_O + xb_{Cl}\}[a_{ClH}(Q)-1] \\ & +(1-x)b_O/\{(1-x)b_O + xb_{Cl}\}[a_{OH}(Q)-1]. \end{aligned} \quad (14)$$

The intermolecular interference term for the sample of "null mixture" is directly connected with the sum of contributions from O–O, Cl–Cl, and Cl–O pairs,

$$\begin{aligned} & (d\sigma/d\Omega)_{int}^{inter}(\text{for } ^0H) = (1-x)^2 b_O^2[a_{OO}(Q)-1] + x^2 b_{Cl}^2[a_{ClCl}(Q)-1] \\ & \quad +2x(1-x)b_O b_{Cl}[a_{ClO}(Q)-1] \\ & = \{xb_{Cl} + (1-x)b_O\}^2[a_{XX}(Q)-1], \end{aligned} \quad (15)$$

where

$$\begin{aligned} a_{XX}(Q)-1 = {} & (1-x)^2 b_O^2/\{xb_{Cl} + (1-x)b_O\}^2[a_{OO}(Q)-1] \\ & +x^2 b_{Cl}^2/\{xb_{Cl} + (1-x)b_O\}^2[a_{ClCl}(Q)-1] \\ & +2x(1-x)b_O b_{Cl}/\{xb_{Cl} + (1-x)b_O\}^2[a_{ClO}(Q)-1]. \end{aligned} \quad (16)$$

The intermolecular distance, root mean square amplitude of i–j pair and coordination number of j atoms around i atom, r_{ij}, l_{ij}, and n_{ij}, are respectively determined by the least-squares fit of observed partial structure factors to the corresponding theoretical ones $a_{ij}^{calc}(Q)$, which involve the contribution from the long-range random distribution of atoms as below:[6,44,45]

$$\begin{aligned} a_{ij}^{calc}(Q) = {} & \sum \beta_{ij} n_{ij} \exp(-l_{ij}^2 Q^2/2) \sin(Qr_{ij})/(Qr_{ij}) \\ & +4\pi\rho \exp(-l_{0ij}^2 Q^2/2)[Qr_{0ij}\cos(Qr_{0ij}) - \sin(Qr_{0ij})]Q^{-3}, \end{aligned} \quad (17)$$

where ρ gives the number density of the stoichiometric unit $(HCl)_x(H_2O)_{1-x}$. The parameter, r_{0ij}, denotes the distance beyond which the uniform distribution of j atoms around i atom is assumed and l_{0ij} means the sharpness of the boundary at r_{0ij}. The coefficient β_{ij} in Eq. 17 is written as

$$\beta_{HH} = (2-x)^{-1}, \quad (18)$$

and

$$\beta_{XH} = \gamma_{XH}[(2-x)\{(1-x)b_O + xb_{Cl}\}]^{-1}, \quad (19)$$

where $\gamma_{OH} = (1-x)b_O$ and $\gamma_{ClH} = xb_{Cl}$,

and

$$\beta_{XX} = \delta_{XX}[(1-x)b_O + xb_{Cl}]^{-2}. \quad (20)$$

Here $\delta_{OO} = (1-x)b_O^2$, $\delta_{ClCl} = xb_{Cl}^2$, and $\delta_{ClO} = 2xb_{Cl}b_O$. The fitting procedure was made in the range of $0.33 \le Q \le 9.78$ Å^{-1} using the SALS program.[42]

The partial distribution function, $g_{ij}(r)$, is represented as the Fourier transform of the observed $a_{ij}(Q)$:

$$g_{ij}(r) = 1 + (2\pi^2\rho r)^{-1} \int_0^{Q_{max}} Q\,[a_{ij}(Q) - 1]\mathrm{d}Q. \quad (21)$$

The upper limit, Q_{max}, in the integral was taken to be 9.78 Å^{-1}.

Results and Discussion

Liquid Pure Water. The observed cross sections, $(\mathrm{d}\sigma/\mathrm{d}\Omega)^{obs}$, for three H_2O–D_2O mixtures with different H/D ratios are shown in Fig. 1a. A marked difference in the neutron diffraction patterns is seen among these mixtures. The decrease in the intensity of $(\mathrm{d}\sigma/\mathrm{d}\Omega)^{obs}$ at a larger-Q range due to the inelasticity effect, becomes more pronounced for H-richer mixtures. On the other hand, the observed intermolecular interference function, $(\mathrm{d}\sigma/\mathrm{d}\Omega)^{inter}_{int}$, for these mixtures in Fig. 1b preferably oscillates around the asymptotic value 0, although some differences in the amplitude of $(\mathrm{d}\sigma/\mathrm{d}\Omega)^{inter}_{int}$ due to that in the mean coherent scattering length of H are found among these solutions. The functional form of the present $(\mathrm{d}\sigma/\mathrm{d}\Omega)^{inter}_{int}$ for 99.9% D_2O is almost identical to that reported in the previous neutron diffraction studies.[43,46,47]

Partial structure factors: $a_{HH}(Q)$, $a_{OH}(Q)$, and $a_{OO}(Q)$ obtained by the combination of the observed $(\mathrm{d}\sigma/\mathrm{d}\Omega)^{inter}_{int}$ through Eqs. 9, 11, and 15, are given in Fig. 2. The usual procedure has been to deduce structural parameters for the nearest-neighbor atomic pair from the partial distribution function, $g_{ij}(r)$, which can be derived by the Fourier transform of the observed $a_{ij}(Q)$. However, because of the limited observable Q-range (Q_{max}=9.78 Å^{-1}) and relatively large statistical uncertainties in the observed $a_{ij}(Q)$, we determine

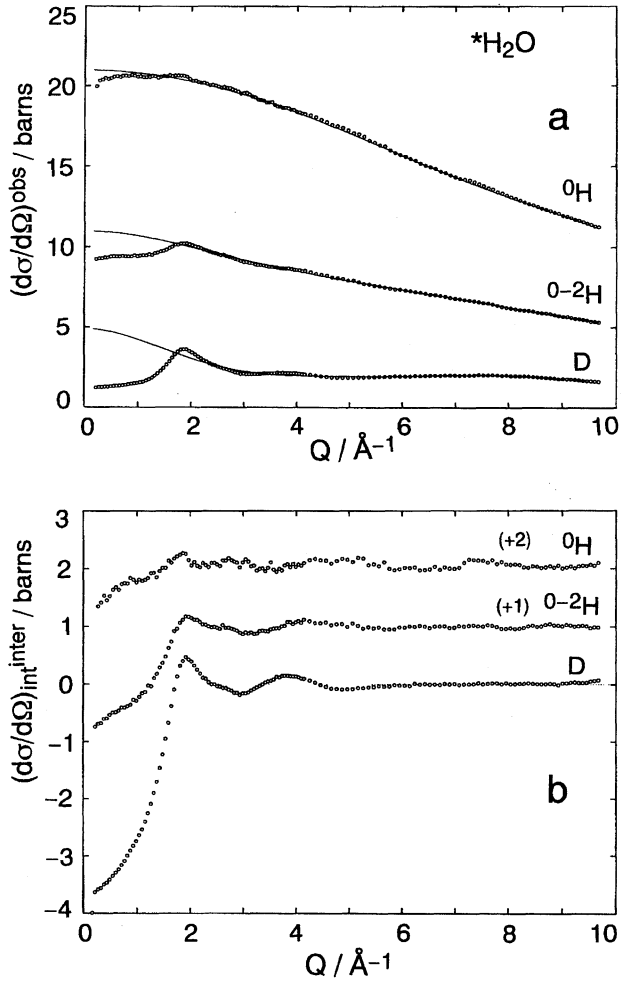

Fig. 1. a) Observed single+multiple scattering cross sections, $(\mathrm{d}\sigma/\mathrm{d}\Omega)^{obs}$, for liquid pure water with the different isotopic ratio of H/D (circles). Calculated intramolecular+self scattering contributions are indicated by solid lines. b) Observed intermolecular interference terms $(\mathrm{d}\sigma/\mathrm{d}\Omega)^{inter}_{int}$ (circles).

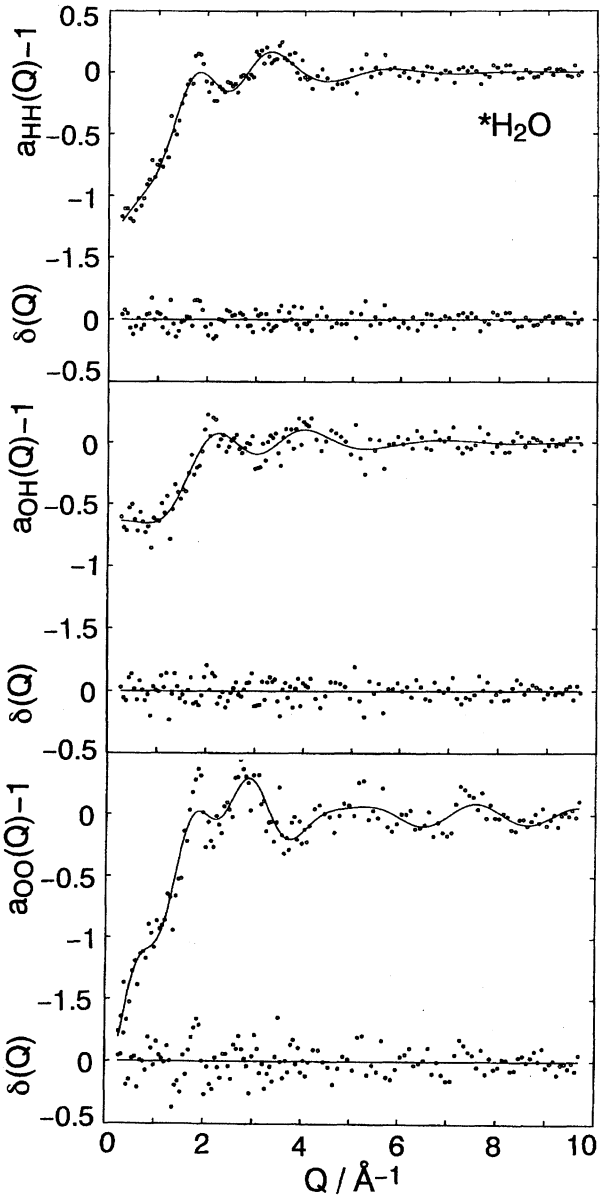

Fig. 2. Circles: Observed H–H, O–H, and O–O partial structure factors $a_{ij}(Q)$ for liquid pure water. Solid lines: The best-fit of calculated interference terms in Eq. 17. The difference between observed and calculated $a_{ij}(Q)$ is shown below.

these structural parameters by the least-squares fit between the observed $a_{ij}(Q)$ and theoretical one including the long-range random distribution of atoms in Eq. 17. The correction for low-frequency systematic errors in the observed $a_{ij}(Q)$ was applied in advance.[43] In the present fitting procedure, it is assumed that statistical errors distribute uniformly over the whole range of Q covered. While contributions from the first- and the second nearest-neighbor interactions are involved in the theoretical $a_{HH}(Q)$ and $a_{OH}(Q)$, the third-nearest neighbor interaction in the theoretical $a_{OO}(Q)$ is additionally taken into account.

The result of the least squares refinements is summarized in Table 2. The nearest-neighbor H···H distance, r_{HH}=2.39±0.02 Å, is in complete agreement with that reported previously.[48—52] The nearest-neighbor H···H coordination number, n_{HH}=3.9±0.2, is smaller than that obtained earlier (n_{HH}≈6).[48—52] One of the causes for the disagreement may be because the overlapping of the first nearest-neighbor peak and subsequent long-range interactions was ignored in the earlier studies. The nearest-neighbor intermolecular O···H distance, r_{OH}=2.02±0.02 Å, is somewhat larger than that, 1.85 Å, reported by Soper,[48] although the general feature of the present $g_{OH}(r)$ agrees well with that reported in previous works.[48,51,52] The corresponding coordination number, n_{OH}=2.0±0.2, is very close to the literature value, 1.8.[48] The agreement in the value of n_{OH} may show also that the present data correction and normalization procedures are correctly adopted.

A well-defined first peak in $g_{OO}(r)$ in Fig. 3 corresponds to the nearest-neighbor hydrogen-bonded O···O correlation. An additional peak can be found at r≈3.5 Å in the higher-r side of the first peak. The first peak position in $g_{OO}(r)$, 2.8 Å, is in reasonable agreement with that reported for the hydrogen-bonded distance among water molecules by previous X-ray diffraction studies.[9,12,13] The separation of 2.8 and 3.5 Å peaks in the present neutron $g_{OO}(r)$ seems to be more pronounced, compared with the X-ray distribution function previously reported. However, the present $g_{OO}(r)$ has unphysical ripples below the first peak. The period of the ripples, Δr≈0.7 Å, roughly corresponds to the value $\Delta r=2\pi/Q_{max}$=0.64 Å, indicating that they are due to the termination error associated with the Fourier transform. Further, deeper minima at r≈3.0 and 3.9 Å in $g_{OO}(r)$ are supposed also to be due to the termination error. The hydrogen-bonded O···O distance, 2.75±0.02 Å, is slightly shorter than that reported by previous X-ray diffraction studies, 2.85—2.89 Å,[6—14] maybe due to the difference in the scattering mechanism between X-ray and neutron diffrac-

Table 2. Results of the Least-Square Refinement for Partial Structure Factors, $a_{HH}(Q)$, $a_{OH}(Q)$, and $a_{OO}(Q)$, for Pure Liquid Water[a]

		$a_{HH}(Q)-1$	$a_{OH}(Q)-1$	$a_{OO}(Q)-1$
1st nearest neighbor	r_{ij}/Å	2.39(2)	2.02(2)	2.75(2)
	l_{ij}/Å	0.30(1)	0.23(1)	0.13(1)
	n_{ij}	3.9(2)	2.0(2)	2.6(2)
2nd nearest neighbor	r_{ij}/Å	3.96(2)	3.28(2)	3.40(2)
	l_{ij}/Å	0.73(1)	0.52(2)	0.16(2)
	n_{ij}	20(1)	9.5(5)	2.0(2)
3rd nearest neighbor	r_{ij}/Å	—	—	4.46(2)
	l_{ij}/Å	—	—	0.58(1)
	n_{ij}	—	—	11(3)
Long-range interaction	r_0/Å	4.56(5)	3.58(4)	5.02(2)
	l_0/Å	0.81(1)	0.72(3)	0.79(2)

a) Estimated standard deviations are given in parentheses.

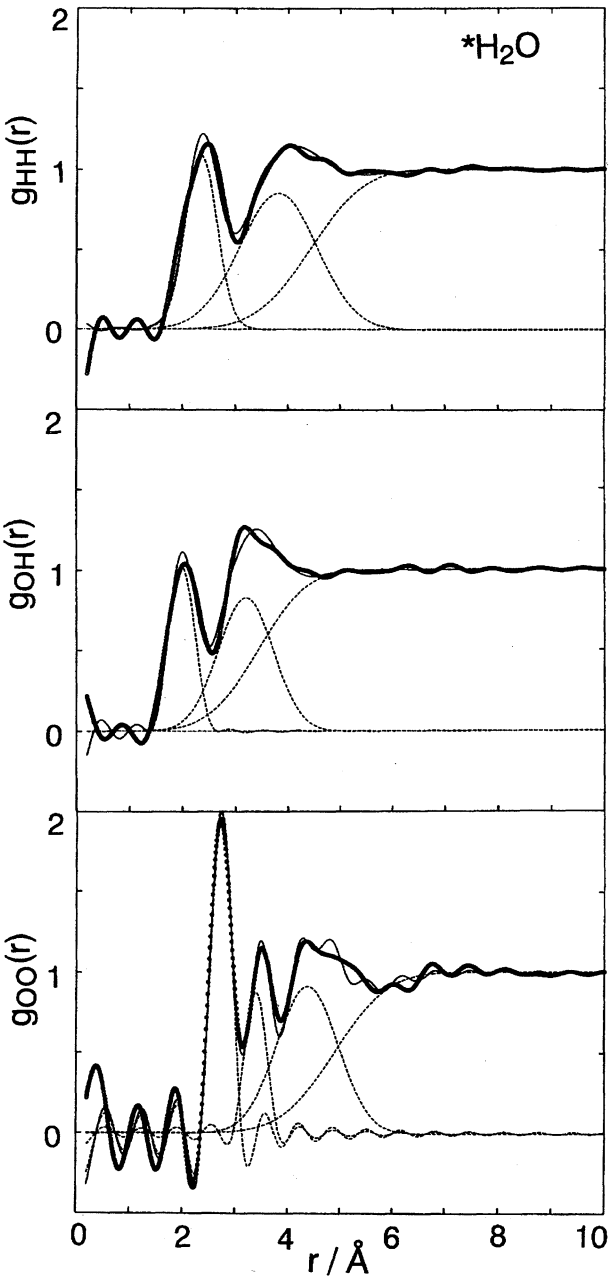

Fig. 3. Circles: Observed H–H, O–H, and O–O partial distribution functions, $g_{ij}(r)$, for liquid pure water. Solid lines: The Fourier transform of the solid lines in Fig. 2. Contributions from both the short-range and long-range interactions are denoted by broken lines.

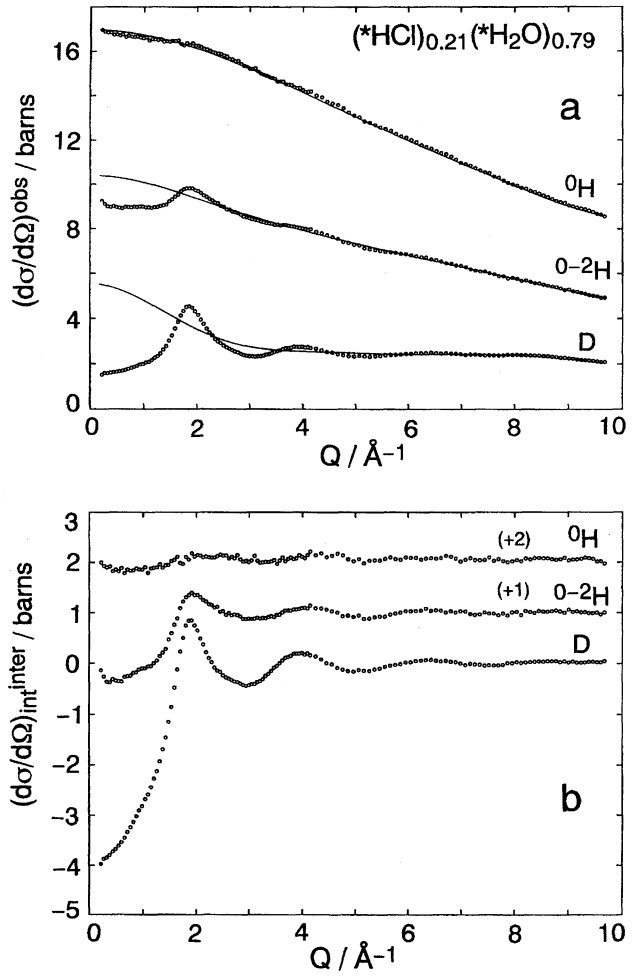

Fig. 4. a) Observed single+multiple scattering cross sections, $(d\sigma/d\Omega)^{obs}$, for aqueous 21 mol% HCl solutions with the different isotopic ratio of H/D (circles). Calculated intramolecular+self scattering contributions are indicated by solid lines. b) Observed intermolecular interference terms, $(d\sigma/d\Omega)_{int}^{inter}$ (circles).

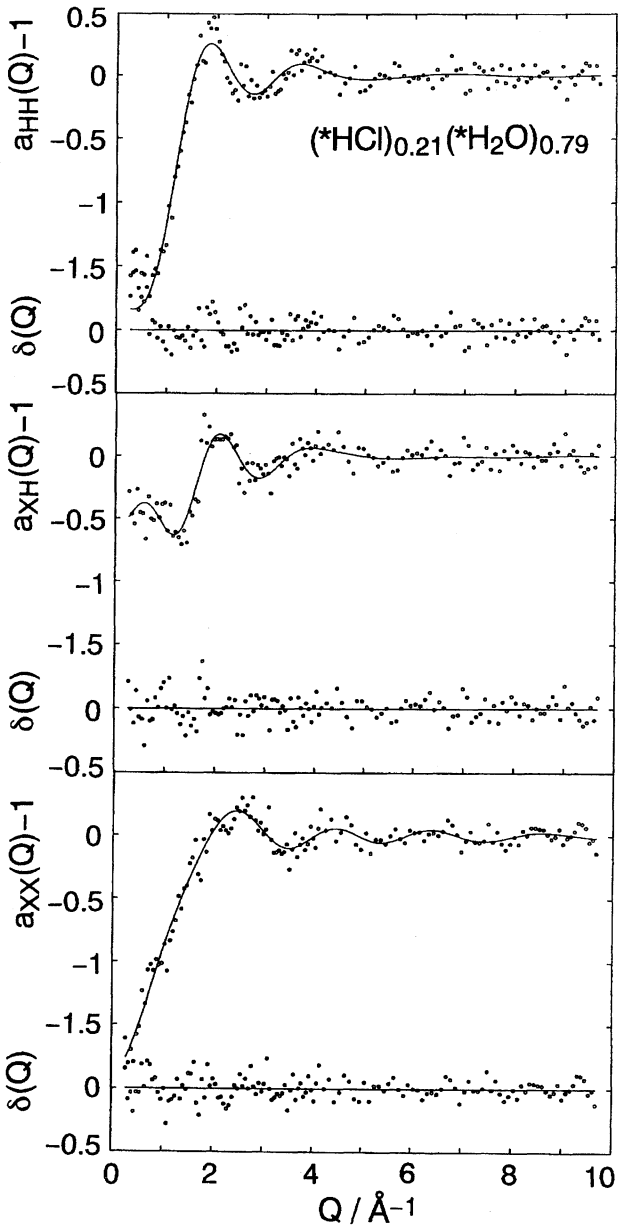

Fig. 5. Circles: Observed H–H, X–H, and X–X (X: O, Cl) partial structure factors, $a_{ij}(Q)$, for the aqueous 21 mol% HCl solution. Solid lines: The best-fit of calculated interference terms in Eq. 17. The difference between observed and calculated $a_{ij}(Q)$ is shown below.

tion methods.[53] The second nearest-neighbor O···O distance, 3.40±0.02 Å, is in good agreement with the value, 3.41 Å, reported by the recent X-ray diffraction study of Yamanaka et al.[13] The sum of the coordination number of the first two nearest-neighbor O–O interactions is estimated to be 4.6±0.4, which agrees well with the value, 4.4, obtained by previous X-ray diffraction studies.[6,10,11,13] These again confirm that the data correction and normalization procedures in the present study have been correctly carried out and that the partial structure factors derived are sufficiently reliable.

Aqueous 21 mol% HCl Solution. The total cross section, $(d\sigma/d\Omega)^{obs}$ and intermolecular interference function, $(d\sigma/d\Omega)_{int}^{inter}$, observed for three HCl solutions with the different H/D isotopic ratio, are shown in Figs. 4a and 4b, respectively. A remarkable difference in $(d\sigma/d\Omega)_{int}^{inter}$ among these solutions appears due to different isotopic compositions. Partial structure factors, $a_{HH}(Q)$, $a_{XH}(Q)$, and $a_{XX}(Q)$, derived by combining the observed $(d\sigma/d\Omega)_{int}^{inter}$ by applying Eqs. 9, 11, and 15, are given in Fig. 5. For the present solutions, $a_{XH}(Q)$ denotes the linear combination of $a_{OH}(Q)$ and $a_{ClH}(Q)$, as described in Eq. 14. $a_{XX}(Q)$ denotes the weighted sum of $a_{OO}(Q)$, $a_{ClCl}(Q)$, and $a_{ClO}(Q)$ (see for example, Eq. 16). The Fourier transforms of $a_{HH}(Q)$, $a_{XH}(Q)$, and $a_{XX}(Q)$ give partial distribution functions: $g_{HH}(r)$, $g_{XH}(r)$, and $g_{XX}(r)$, respectively, which are described in Fig. 6.

The partially resolved first peak located at $r\approx2$ Å in $g_{HH}(r)$, corresponds apparently to the nearest-neighbor intermolecular H···H interaction, the position of which is ca. 0.4 Å shorter than that observed for pure water (ca. 2.4 Å). Therefore, this H···H interaction in the concentrated aqueous HCl solution cannot be explained in term of the formation

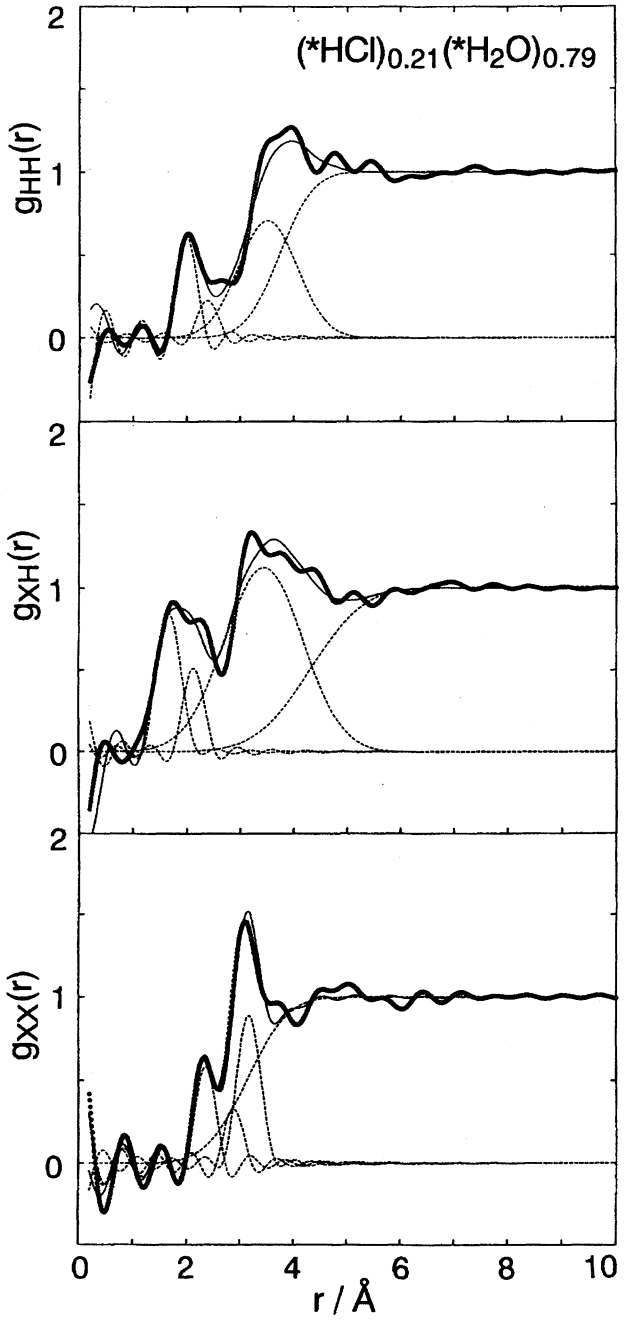

Fig. 6. Circles: Observed H–H, X–H, and X–X (X: O, Cl) partial distribution functions, $g_{ij}(r)$, for the aqueous 21 mol% HCl solution. Solid lines: The Fourier transform of the solid lines in Fig. 4. Contributions from both the short-range and long-range interactions are denoted by broken lines.

of normal hydrogen bonds among H_2O molecules. This shorter H···H interaction can be reasonably assigned to the intermolecular H···H one between H_3O^+ and H_2O molecule, which are strongly hydrogen-bonded to form the protonated water dimer, $H_5O_2^+$, in the solution. A hump in $g_{HH}(r)$ at $r\approx2.5$ Å is judged to have a certain magnitude, maybe corresponding to H···H interactions between H_2O molecules.

Although the first peak position, $r\approx2$ Å, in $g_{XH}(r)$ agrees, in appearance, with that in $g_{OH}(r)$ for liquid pure water, its

Table 3. Results of the Least-Square Refinement for Partial Structure Factors, $a_{HH}(Q)$, $a_{XH}(Q)$, and $a_{XX}(Q)$, for the Aqueous 21 mol% HCl Solution[a)]

		$a_{HH}(Q)-1$	$a_{XH}(Q)-1$	$a_{XX}(Q)-1$
	i–j	H–H	O–H	O–O
1st nearest	r_{ij}/Å	2.02(5)	1.69(2)	2.37(2)
neighbor	l_{ij}/Å	0.13(1)	0.20(1)	0.09(1)
	n_{ij}	0.8(2)	2.0(2)	0.8(1)
	i–j	H–H	Cl–H	O–O
2nd nearest	r_{ij}/Å	2.3(1)	2.14(2)	2.89(2)
neighbor	l_{ij}/Å	0.1(1)	0.14(2)	0.1(1)
	n_{ij}	0.4(2)	4.5(2)	0.6(2)
	i–j	H–H	O*–H[b)]	Cl–O
3rd nearest	r_{ij}/Å	3.6(3)	3.59(2)	3.18(2)
neighbor	l_{ij}/Å	0.54(3)	0.72(1)	0.19(2)
	n_{ij}	10(2)	42(2)	3.5(2)
Long-range	r_0/Å	3.8(2)	4.45(2)	3.24(2)
interaction	l_0/Å	0.5(3)	0.78(1)	0.60(1)

a) Estimated standard deviations are given in parentheses. b) Including both O–H and Cl–H contributions.

asymmetrical peak-shape with a partial splitting may suggest that the peak contains plural interactions. It seems reasonable that contributions from both the nearest-neighbor O···H and Cl···H interactions are involved in the peak. The presence of the nearest-neighbor Cl···O interaction at $r\approx3.2$ Å[2,3,5] has been confirmed according to previous X-ray diffraction studies for concentrated aqueous HCl solutions. In addition, the distance agrees with the Cl···O distance in a variety of aqueous metal-chloride solutions, where H_2O molecules in the first hydration shell point one of the H atoms toward Cl^-. The distance between Cl^- and its nearest-neighbor H atom in such the local configuration has been reported to be 2.23—2.29 Å by neutron diffraction studies.[53,54] Then, we carry out the least-squares fitting analysis for $a_{XH}(Q)$ to determine structural parameters for the H–X interaction under the assumption that contributions from O···H and Cl···H interactions are both involved in the first peak in the $g_{XH}(r)$. The second nearest-neighbor O···H and Cl···H interactions are, of course, involved in the second peak region ($3<r<4$ Å) in the present $g_{XH}(r)$. However, the second nearest-neighbor contributions were treated as a single interaction in the fitting procedure, because the unambiguous decomposition of the second peak is impossible in the present $g_{XH}(r)$.

The X-ray total distribution function for the concentrated HCl solution investigated previously has peaks located at $r\approx2.5$ Å and 3.2 Å.[2,3,5] The present $g_{XX}(r)$ provides similar structural information to the X-ray total distribution function except for the difference in the ratio of scattering amplitudes for O and Cl atoms between the two diffraction techniques. Pronounced short-range peaks are found at $r\approx2.4$ and ≈3.2 Å in the neutron $g_{XX}(r)$ in Fig. 6. These short-range peaks in $g_{XX}(r)$ are attributable to the nearest-neighbor $H_3O^+\cdots H_2O$ and $Cl^-\cdots H_2O$ interactions, respectively. In this result, the nearest-neighbor interactions for

$O(H_3O^+)\cdots O(H_2O)$, $O(H_2O)\cdots O(H_2O)$, and $Cl^-\cdots O(H_2O)$ are added as short-range contributions in the present fitting analysis of $a_{XX}(Q)$.

Results of the least-squares fit for $a_{ij}(Q)$ for the concentrated aqueous HCl solution are summarized in Table 3. The first nearest-neighbor H···H distance, r=2.02±0.05 Å is considerably shorter than that obtained for liquid pure water (2.39±0.02 Å). Recent ab initio MD simulation has revealed that the first peak position in $g_{HH}(r)$ for pure water significantly shifts toward a lower-r side by ca. 0.5 Å in the aqueous solution with excess protons.[22] This shorter interatomic distance has been pointed out to correspond to the H···H distance within the protonated water dimer, $H_5O_2^+$.[22,24,25] Therefore, the present shorter H···H interaction may suggest the formation of $H_5O_2^+$ in the concentrated 21 mol% HCl solution. The second nearest-neighbor H···H distance, 2.3±0.1 Å obtained from the fitting of $a_{HH}(Q)$ corresponds well to that in Table 2 obtained for pure water (2.39 Å), implying that this H···H interaction is ascribed by the nearest-neighbor $H_2O\cdots H_2O$ correlation. The nearest-neighbor O···H distance, 1.69±0.02 Å, is ca. 0.3 Å shorter than that obtained for pure water, suggesting the presence of the extremely strong hydrogen bond in the concentrated aqueous HCl solution. The Cl···H distance, 2.14±0.02 Å, is ca. 0.1 Å shorter than that from the neutron diffraction measurement with the $^{35}Cl/^{37}Cl$ isotopic substitution in various aqueous metal-chloride solutions (2.22—2.29 Å).[54,55] This points out that further neutron diffraction measurements with the $^{35}Cl/^{37}Cl$ isotopic substitution are necessary for obtaining more detailed structural information concerning the Cl···H interaction in the concentrated aqueous HCl solution. This will be a future subject for research.

The nearest neighbor O···O distance, 2.37±0.02 Å, for the present HCl solution determined by the least-squares fit to the observed $a_{XX}(Q)$, is much shorter than that obtained for pure water. This short intermolecular distance is in good agreement with the hydrogen-bonded O···O distance within the $H_5O_2^+$ structural unit found in crystalline hydrates, such as $HCl{\cdot}2H_2O$ (2.41 Å)[56] and $HCl{\cdot}3H_2O$ (2.43 Å).[57] This shows the possibility that the hydrogen bond between H_3O^+ and its nearest-neighbor H_2O molecules is very strong to form such the structural unit in the highly concentrated HCl solution. The second nearest-neighbor O···O distance, 2.89±0.02 Å, in Table 3 can be assigned to the hydrogen-bonded $O(H_2O)\cdots O(H_2O)$ interaction. The nearest-neighbor Cl···O distance, 3.18±0.02 Å, in Table 3 is roughly identical to that, 3.10—3.20 Å,[53] reported for various aqueous metal chloride solutions. It appears that each Cl^- in the 21 mol% HCl solution is surrounded by, on the average, four O atoms which belong to its nearest-neighbor H_2O or $H_5O_2^+$ molecules.

The formation of hydrogen-bonded bi-chloride species, Cl–H···Cl, as predicted by the ab initio MD calculation,[23] could not be proved in the present study. The combination of the $^{35}Cl/^{37}Cl$ isotopic substitution experiment and the second-order difference method in the neutron diffraction measurement[58,59] will provide the Cl–Cl partial distribution function, $g_{ClCl}(r)$. This will also be researched in the near future.

The authors wish to thank Professor Noam Agmon (Hebrew University) for helpful discussions. We would like to thank The Institute of Solid State Physics (ISSP), the University of Tokyo, for providing us to use the diffractometer PANSI installed at JRR-2 research reactor. The authors are also grateful to Professor Hideki Yoshizawa (the University of Tokyo) and Mr. Yoshihisa Kawamura (the University of Tokyo) for their help during the course of the neutron diffraction measurements. All of the calculations were carried out with the S-4/1000 computer at the Computing Center of Yamagata University. This work was partially supported by a Grant-in-Aid for Scientific Research No. 09640657 from the Ministry of Education, Science, Sports and Culture.

References

1) T. Bountis, "Proton Transfer in Hydrogen-Bonded Systems," Plenum Press, New York (1992).
2) S. C. Lee and R. Kaplow, *Science*, **169**, 477 (1970).
3) D. L.Weltz, *J. Solution Chem.*, **1**, 489 (1972).
4) H.-G. Lee, Y. Matsumoto, T. Yamaguchi, and H. Ohtaki, *Bull. Chem. Soc. Jpn.*, **56**, 443 (1983).
5) R. Triolo and A. H. Narten, *J. Chem. Phys.*, **63**, 3624 (1975).
6) A. H. Narten, M. D. Danford, and H. A. Levy, *Discuss. Faraday Soc.*, **43**, 97 (1967).
7) A. H. Narten and H. A. Levy, *J. Chem. Phys.*, **55**, 2263 (1971).
8) A. H. Narten, *J. Chem. Phys.*, **56**, 5681 (1972).
9) F. Hajdu, S. Lengyel, and G. Pálinkás, *J. Appl. Cryst.*, **9**, 134 (1976).
10) G. A. Gaballa and G. W. Neilson, *Mol. Phys.*, **50**, 97 (1983).
11) R. Coban and M. D. Zeidler, *Ber. Bunsenges. Phys. Chem.*, **96**, 1463 (1992).
12) A. V. Okhulkov, Yu. N. Demianets, and Yu. E. Gorbaty, *J. Chem. Phys.*, **100**, 1578 (1994).
13) K. Yamanaka, T. Yamaguchi, and H. Wakita, *J Chem. Phsy.*, **101**, 9830 (1994).
14) T. Radnai and H. Ohtaki, *Mol. Phys.*, **87**, 103 (1996).
15) M. De Paz, S. Ehrenson, and L. Friedman, *J. Chem. Phys.*, **52**, 3362 (1970).
16) M. D. Newton and S. Ehrenson, *J. Am. Chem. Soc.*, **93**, 4971 (1971).
17) S. Scheiner, *J. Am. Chem. Soc.*, **103**, 315 (1981).
18) Y. Xie, R. B. Remington, and H. F. Schaefer, III, *J. Chem. Phys.*, **101**, 4878 (1994).
19) D. Wei and D. R. Salahub, *J. Chem. Phys.*, **101**, 7633 (1994).
20) T. Komatsuzaki and I. Ohmine, *Chem. Phys.*, **180**, 239 (1994).
21) N. Laurs and P. Bopp, *Ber. Bunsenges. Phys. Chem.*, **97**, 982 (1993).
22) J. Lobaugh and G. A. Voth, *J. Chem. Phys.*, **104**, 2056 (1996).
23) K. E. Laasonen and M. L. Klein, *J. Phys. Chem. A*, **101**, 98 (1997).
24) N. Agmon, *J. Mol. Liq.*, **73/74**, 513 (1997).
25) N. Agmon, *J. Phys. Chem. A*, **102**, 192 (1998).
26) V. F. Sears, "Thermal-Neutron Scattering Lenghts and Cross

Sections for Condensed Matter Research," AECL-8490, Atomic Energy of Canada Ltd., (1984), p. 16.
27) J. G. Powles, *Adv. Phys.*, **22**, 1 (1973).
28) J. R. Granada, V. H. Gillete, and R. E. Mayer, *Phys. Rev. A*, **36**, 5594 (1987).
29) H. H. Paalman and C. J. Pings, *J. Appl. Phys.*, **33**, 2635 (1962).
30) I. A. Blech and B. L. Averbach, *Phys. Rev.*, **137**, A1113 (1965).
31) H. Bertagnolli, P. Chieux, and H. G. Hertz, *Ber. Bunsenges. Phys. Chem.*, **88**, 977 (1984).
32) G. Placzek, *Phys. Rev.*, **86**, 377 (1952).
33) J. G. Powles, *Mol. Phys.*, **37**, 623 (1979).
34) M. Rovere, L. Blum, and A. H. Narten, *J. Chem. Phys.*, **73**, 3729 (1984).
35) J. G. Powles, *Mol. Phys.*, **42**, 757 (1981).
36) J. R. Granada, *Phys. Rev. B*, **31**, 4167 (1985).
37) D. G. Montague, I. P. Gibson, and J. C. Dore, *Mol. Phys.*, **44**, 1355 (1981).
38) D. G. Montague and J. C. Dore, *Mol. Phys.*, **57**, 1035 (1986).
39) D. G. Montague, I. P. Gibson, and J. C. Dore, *Mol. Phys.*, **47**, 1405 (1982).
40) D. C. Chanpeney, R. N. Joarder, and J. C. Dore, *Mol. Phys.*, **58**, 337 (1986).
41) M.-C. Bellissent-Funel, L. Bosio, and J. Texeira, *J. Phys.: Condens. Matter*, **3**, 4065 (1991).
42) T. Nakagawa and Y. Oyanagi, "Recent Development in Statistical Inference and Data Analysis," ed by K. Matushita, North-Holland (1980), p. 221.
43) Y. Kameda and O. Uemura, *Bull. Chem. Soc. Jpn.*, **65**, 2021 (1992).
44) R. Caminiti, P. Cucca, M. Monduzzi, G. Saba, and G. Crisponi, *J. Chem. Phys.*, **81**, 543 (1984).
45) H. Ohtaki and N. Fukushima, *J. Solution Chem.*, **21**, 23 (1992).
46) I. P. Gibson and J. C. Dore, *Mol. Phys.*, **48**, 1019 (1983).
47) D. C. Steytler and J. C. Dore, *Mol. Phys.*, **56**, 1001 (1985).
48) A. K. Soper, *Chem. Phys.*, **107**, 61 (1986).
49) A. K. Soper, *J. Chem. Phys.*, **101**, 6888 (1994).
50) A. K. Soper and R. N. Silver, *Phys. Rev. Lett.*, **49**, 471 (1982).
51) P. Postorino, M. A. Ricci, and A. K. Soper, *J. Chem. Phys.*, **101**, 4133 (1994).
52) A. K. Soper, F. Bruni, and M. A. Ricci, *J. Chem. Phys.*, **106**, 247 (1997).
53) H. Ohtaki and T. Radnai, *Chem. Rev.*, **93**, 1157 (1993).
54) S. Cummings, J. E. Enderby, G. W. Neilson, J. R. Newsome, R. A. Howe, W. S. Howells, and A. K. Soper, *Nature*, **287**, 714 (1980).
55) D. H. Powell, A. C. Barnes, J. E. Enderby, G. W. Neilson, and P. S. Salmon, *Faraday Discuss. Chem. Soc.*, **85**, 137 (1988).
56) J-O. Lindgren and I. Olovsson, *Acta Crystallogr.*, **23**, 966 (1967).
57) J-O. Lindgren and I. Olovsson, *Acta Crystallogr.*, **23**, 971 (1967).
58) G. W. Neilson and J. E. Enderby, *Proc. R. Soc. London*, **A390**, 353 (1983).
59) G. W. Neilson, R. D. Broadbent, I. Howell, and R. H. Tromp, *J. Chem. Soc., Faraday Trans.*, **89**, 2927 (1993).